On conductivity, permittivity, apparent diffusion coefficients and their use as cancer markers at MRI frequencies

Ileana Hancu[1], Jeanette Roberts[1], Seung-Kyun Lee[1], Robert Lenkinski[2], and Selaka Bulumulla[1]
[1]*GE Global Research Center, Niskayuna, NY, United States,* [2]*UT Southwestern Medical Center, TX, United States*

Target Audience: Researchers/clinicians interested in conductivity, permittivity and ADC measurements by MRI and their value as cancer markers

Introduction: Recent demonstration of tissue electrical properties (TEP) mapping by MRI [1] has raised hopes that these parameters can increase the specificity of cancer detection. Given the current limitations of MRI based TEP measurements, and tumor to normal ratios of conductivity and permittivity reports varying between 1.1 [2] and 5[3], it is important to quantify the tumor/normal TEP differences by gold standard measurements. Moreover, verification of the suggested linear relationship between apparent diffusions coefficient (ADC) and conductivity [4] is also interesting to explore, to clarify the potential of TEP's as independent markers of disease. Here, conductivity and permittivity measurements were performed in two rat tumor models using an impedance analyzer and a dielectric probe over the 50-270MHz range. Correlations between tumor conductivity and ADC's (measured at 3T) were also performed. Recommendations regarding field strength and MRI based TEP mapping capability are offered.

Methods: A. Tumor models and impedance analyzer based dielectric measurements: Cells from the MATBIII (breast adenocarcinoma) and MATLyLu (prostate carcinoma) tumor lines were implanted in the flanks of 6 Fisher and 7 Copenhagen rats. When tumors reached a size of ~8cc, they were imaged; the skin was then opened, and an E4991 impedance analyzer/E85070 dielectric probe (Agilent, USA) were used for dielectric measurements over the 50-270MHz range. 4-6 such measurements were performed in different places of the tumor and normal muscle, to increase measurement accuracy and compensate for the non-isotropic sensitivity of the dielectric probe in its sample volume of ~8cc.

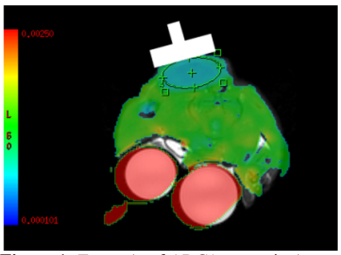

Figure 1: Example of ADC/ anatomical overlay, with dielectric probe (white)

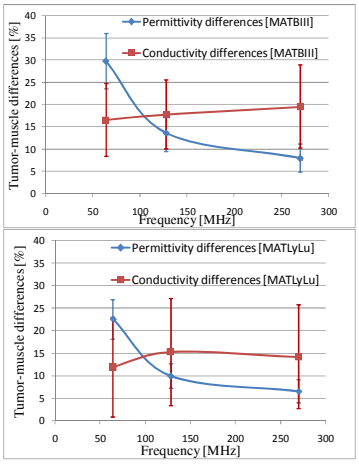

Figure 2: Tumor-muscle TEP differences for the MATBIII (top) and MATLyLu (bottom) strains as a function of frequency

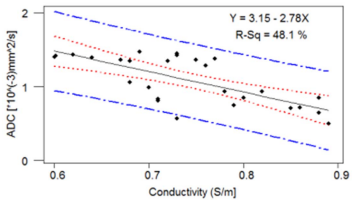

Figure 3: Correlation between ADC and conductivity at 128MHz.

B. MRI measurements: A 3T, GE MR750 scanner (Waukesha, WI), and a quadrature transmit receive Litzcage coil (Doty Scientific) were used for all imaging experiments. Thirteen slices were acquired in the diffusion weighted acquisition, at 1/1.5mm in/through plane spatial resolution, b values of 0 and 600 $*10^{-3}mm^2/s$, TE/TR=52/4000ms, for a total acquisition time of 3:48. Average ADC's over the tumor and adjacent muscle were computed and used to correlate with the probe-based conductivity measurements.

C. Data analysis: SPSS 19 was used for all statistical analysis. Linear regression between the conductivity measurements and averaged ADC values (each obtained for 13 muscle/13 tumor tissues) was performed to understand the linearity of these two variables. Assuming that ADC values are field independent, stepwise discriminant analysis was also carried out, and discriminant functions were computed that best separated muscle from tumor at 64, 128 and 270MHz, respectively. To select predictors, Wilk's lambda method was employed. An F-statistic was used to threshold entering/exiting variables; the criteria for entry was an F-function probability of 0.05, and the criteria for removal was a F-function probability of 0.1.

Results: Figure 1 shows an overlay between the ADC image and the anatomical image, with the tumor region encircled by the green elliptical ROI; the dielectric probe placement (after the MRI exam) is also exemplified here. Figure 2 displays the TEP's tumor-muscle differences in the MATBIII/MATLyLu tumors (top/bottom) as a function of frequency; the standard deviations reported are between animals. While some differences exist, the range of contrasts seen in the 2 tumor strains are similar, varying, e.g., between 0 and 30% in conductivity and between 15 and 30% in permittivity at 64MHz. Decreasing permittivity contrast and somewhat constant conductivity contrast is seen progressing from 64, to 128 and to 270MHz. Figure 3 displays the correlation between ADC's and the probe-based conductivity measurements at 128MHz. While higher ADC is associated with lower conductivity, the linear fit explains only a limited fraction of data variability (R^2=0.48). Following stepwise discriminant analysis at the 3 frequencies, Table 1 shows the standardized canonical discrimination function coefficients and Wilk's lambda (defining the proportion of the total variance in the discriminant scores not explained by differences among the groups). As coefficients with large absolute values correspond to variables with greater discriminating ability- the field strength dependence of TEP's imparts a strong weight on the capability of different factors to help discriminate between cancer an normal tissue. While permittivity has the strongest discrimination power at 1.5T, is becomes comparable to ADC at 3T, and less important than ADC at 7T. Conversely, conductivity measurements impart limited or no incremental discrimination power above ADC; note that even at 128MHz, if only ADC and conductivity are entered as independent variables in the discriminant analysis, only ADC ends up part of the discriminant function. Whether this is due to the ADC correlation to conductivity, or to the high intra-subject (7%/4% for conductivity/ permittivity) and inter-subject variability (11%/8% for conductivity/permittivity) remains to be determined.

Conclusions: This study offers insight into the requirements for MRI based TEP mapping. While human tumors may differ from the tumors studied here, the limited TEP differences between normal tissue and tumors are likely to persist. Measurement accuracy/repeatability similar to the one exhibited by the dielectric probe need to be developed for MRI based TEP mapping, for these parameters to offer additional discriminatory power for cancer detection. Our results also suggest that ADC, in combination with lower field permittivity measurements may provide a better combination for increasing cancer detection specificity. Balancing our results with the better capability of higher field strength for permittivity measurements [5], it is likely that 3T would offer the best compromise between higher measurement capability and bigger permittivity differences.

Frequency [MHz]	ADC	Permittivity	Conductivity
64 (0.04)	-0.7 (0.15)	0.9 (0.07)	0 (0.6)
128 (0.06)	-1 (0.15)	1 (0.19)	0.6 (0.6)
270 (0.09)	0.9 (0.15)	-0.7 (0.35)	0 (0.6)

Table 1: Standardized canonical discrimination function coefficients. Wilk's lambdas are displayed in parantheses, for each variable separately, and for the combined discriminant function (under the Frequency column)

Acknowledgement: This work was supported by NIH grant 1R01CA154433.

References: [1] Bulumulla et al, Concepts Magn Reson Med 41B(1):13 (2012) [2] Lazebnik et al, Phys Med Biol, 52(10):2637 (2007) [3] Joines et al, Med Phys (21)4: 547 (1994) [4] Tuch et al. PNAS, 98(20):11697 (2001) [5] A. van Lier at al, Proc Intl Soc Magn Reson Med 19:125 (2011).